The EMBO Journal Vol.18 No.23 pp.6752–6761, 1999

Two activities of cofilin, severing and accelerating directional depolymerization of actin filaments, are affected differentially by mutations around the actin-binding helix

Kenji Moriyama and Ichiro Yahara[1]

Department of Cell Biology, The Tokyo Metropolitan Institute of Medical Science, Honkomagome, Bunkyo-ku, Tokyo 113-8613, Japan

[1]Corresponding author
e-mail: yahara@rinshoken.or.jp

The biochemical activities of cofilin are controversial. We demonstrated that porcine cofilin severs actin filaments and accelerates monomer release at the pointed ends. At pH 7.1, 0.8 μM cofilin cut filaments (2.2 μM actin) about every 290 subunits and increased the depolymerization rate 6.4-fold. A kink in the major α-helix of cofilin is thought to constitute a contact site for actin. Side chain hydroxyl groups of Ser119, Ser120 and Tyr82 in cofilin form hydrogen bonds with main chain carbonyl moieties from the helix, causing the kink. We eliminated side chain hydroxyls by Ser→Ala and/or Tyr→Phe mutagenesis. Severing and depolymerization-enhancing activities were reduced dramatically in an Ala120 mutant, whereas the latter was decreased in a Phe82 mutant with a relatively small effect on severing, suggesting different structural bases for the two activities of cofilin. The Ala120-equivalent mutation in yeast cofilin affected cell growth, whereas that of the Phe82-equivalent had no effect in yeast. These results indicate the physiological significance of the severing activity of cofilin that is brought about by the kink in the helix.
Keywords: actin/cofilin/mutation/tertiary structure/yeast

Introduction

Cofilin (or ADF) is a low molecular weight actin-regulating protein that is ubiquitous among eukaryotes. Cofilin functions in cytokinesis, endocytosis and various other motile processes involving actin dynamics (Abe *et al*., 1996; Aizawa *et al*., 1996; Carlier *et al*., 1997; Lappalainen and Drubin, 1997; Rosenblatt *et al*., 1997). The strict necessity for cofilin for viability in yeast, slime mould, nematode and fruit fly indicates its biological importance (Iida *et al*., 1993; Moon *et al*., 1993; McKim *et al*., 1994; Aizawa *et al*., 1995; Gunsalus *et al*., 1995). The biochemical activities responsible for its essential biological role, however, have remained controversial. Because subunits are exchanged exclusively at the ends of actin filaments, the dynamics of uncapped filaments should be enhanced by accelerating subunit flux in the filaments (treadmill), and/or by filament fragmentation to increase the number of filament ends (severing). Either event should augment the rate of subunit exchange between F-actin and the monomeric actin pool, resulting in enhanced actin dynamics. Evidence has been presented for both treadmill and severing mechanisms with respect to cofilin. Classical studies have regarded enhanced rates of elongation and disassembly of uncapped F-actin as evidence of fragmentation, and this interpretation has been applied to cofilin action (Nishida *et al*., 1985; Maciver *et al*., 1991; Moon *et al*., 1993). However, Carlier and her associates argued that all the effects of cofilin could be attributed to the treadmill model, and refuted the notion of actin-severing activity (Carlier *et al*., 1997). Several recent reports have also supported the treadmill model (Lappalainen and Drubin, 1997; Rosenblatt *et al*., 1997). In this study, we critically examined both models of cofilin action on actin.

The three-dimensional structures of cofilin and its homologues have notable features. The tertiary structure of cofilin is strikingly similar to segments of gelsolin, an actin-severing/capping protein, although the primary structure has no significant homology (Hatanaka *et al*., 1996; Fedorov *et al*., 1997; Leonard *et al*., 1997). Like gelsolin segment 1, cofilin is thought to use a long helix to make immediate contact with actin. This view is supported by biochemical data (Yonezawa *et al*., 1989, 1991; Moriyama *et al*., 1992; Wriggers *et al*., 1998). The actin-binding helix of cofilin is kinked around the middle, whereas no irregularity is apparent in gelsolin segment 1 (McLaughlin *et al*., 1993). Thus, the kink in the structure of cofilin may have functional significance. Possible causes of the irregular fold in the cofilin helix have been indicated by two X-ray crystallographic studies (Fedorov *et al*., 1997; Leonard *et al*., 1997) and our NMR data (H.Hatanaka and K.Moriyama, unpublished works). The results of these studies suggest that three side chain to main chain hydrogen bonds interrupt the normal α-helix fold through disrupting intra-backbone hydrogen bonding. Since the side chain proton donors could be hydroxyl moieties of Ser119, Ser120 and Tyr82 in mammalian cofilin, we created porcine cofilin mutants in which these amino acids were replaced by Ala119, Ala120 and Phe82, respectively, then determined the functional significance of the triad of hydrogen bonds.

Results

Cofilin severs actin filaments

The rate of F-actin depolymerization is measured conventionally by initiating its disassembly by dilution or by adding avid actin monomer-sequestering proteins. The amount of residual F-actin is then determined spectrophotometrically as a function of time, and the rate of depolymerization is calculated (Walsh *et al*., 1984; Maciver *et al*., 1991; Weber *et al*., 1994). To determine both the severing and disassembly of F-actin simultaneously as a function of time, we modified this method as follows. We assumed that the depolymerization rate of F-actin depends on the dissociation rate from the pointed end and the number of free pointed ends. We examined whether or

not these two parameters are altered depending on the concentration of porcine cofilin.

When actin is polymerized in the presence of a limited amount of gelsolin, the concentration (number per unit volume) of the resulting filaments is almost equal to that of gelsolin, because the filaments are nucleated exclusively by gelsolin (Bryan and Coluccio, 1985; Janmey *et al*., 1986; Weber *et al*., 1994). Gelsolin-capped filaments were incubated with cofilin in the presence of gelsolin–actin dimers. The binary complexes were added simultaneously with cofilin, so as to cap newly formed free barbed ends. F-actin depolymerization was then initiated by vitamin D-binding protein (DBP), a potent actin monomer- sequestering protein. The rate of disassembly at pointed ends was estimated from time-dependent depolymerization. When the initial rate is plotted versus the initial concentration of gelsolin, the slope of a linear regression line represents an off-rate constant at the pointed end and the intercept on the abscissa represents an alteration in the filament number per unit volume. Thus, a negative intercept value indicates that cofilin severs F-actin to increase the filament concentration.

However, the binding of cofilin to F-actin itself significantly increases light scattering and the turbidity of the solution, and it also partially quenches fluorescence of the pyrene attached to actin in the polymer (Nishida *et al*., 1984; Carlier *et al*., 1997). To circumvent these difficulties, we initiated F-actin depolymerization when a new steady-state of the F-actin solution regarding pyrene fluorescence was achieved after adding cofilin (Figure 1A). The amount of unpolymerized actin at the new steady-state was determined by a DNase I inhibition assay and the amount of F-actin per fluorescence unit was calculated for each reaction with cofilin. According to this protocol, the decrease in the fluorescence intensity closely approximates the amount of depolymerized actin, within the range of cofilin concentrations used in the experiments shown in Figure 1. Pyrene fluorescence was quenched maximally at 8.7% in the presence of 0.8 μM His_6-tagged cofilin. We first calibrated the time of pre-incubation with cofilin prior to DBP addition, because whether severing of F-actin by cofilin is fast or slow (and catalytic or stoichiometric) was unknown. One example is shown in Figure 1B, in which the rate constant was plotted against the pre-incubation time when 16.3 nM gelsolin-nucleated filaments were reacted with 0.3 μM cofilin. The rate constants were derived from the DBP-induced disassembly traces assuming exponential kinetics. We found that the rate constant slowly increased initially, suggesting an increase in the number of filament ends due to severing. However, the increase ceased within 10 min, irrespective of the amount of cofilin (0.1–0.8 μM). This suggests that cofilin severs F-actin in a 'slow and stoichiometric' fashion and not catalytically. Based on these results, we set 10 min as the pre-incubation time and measured all the severing events during this period.

Traces of DBP-induced fluorescence changes are shown in Figure 1C for F-actin reacted beforehand with 0.8 μM wild-type cofilin. The rate constants for the depolymerization reactions were calculated by applying exponential curve fits, because they closely followed exponential kinetics (Figure 1D). We then plotted calculated off-rates (at time = 0) versus initial concentrations of gelsolin (number of filaments) (Figure 1E). The results show that cofilin increased both the slope and the number of filament ends, suggesting that cofilin severs filaments and accelerates subunit dissociation from the pointed end. Similar experiments were performed using 0.1, 0.3 and 0.5 μM cofilin. From these data, we calculated a frequency of one cut per 290 actin subunits and a 6.4-fold increase in the dissociation rate constant at pointed ends in the presence of 0.8 μM cofilin.

To obtain more evidence of severing, we observed fluorescently labelled F-actin under an epifluorescence microscope after reaction with cofilin within 1 min (Figure 2). The results showed that cofilin shortened filaments and increased the number of them in a concentration-dependent manner (Figure 2). This suggests that cofilin severed Alexa-labelled F-actin. It is unlikely that the increased number of filaments can be ascribed to depolymerization and repolymerization rather than to fragmentation of the filaments, because we observed little assembly of monomeric Mg-actin (40% Alexa-labelled) in the presence of cofilin under the same conditions. However, this system required a higher concentration of cofilin than the DBP-induced depolymerization assay to produce significant effects. The difference in the effective concentrations between the two methods may be attributed to the different duration of reaction with cofilin. In addition, F-actin was not capped for the microscopy experiment, whereas gelsolin-capped F-actin was used in the other assay. Despite these differences, both methods demonstrated the actual severing by cofilin.

The role of a triad of hydrogen bonds in the actin-binding helix of cofilin

To examine the functional significance of the triad of hydrogen bonds around the longest α-helix of cofilin, we replaced Tyr82, Ser119 and Ser120 of porcine cofilin with Phe, Ala and Ala, respectively, to eliminate the side chain hydroxyl groups that constitute the proton donors of the triad. Double or triple mutations consisting of these single substitutions were also examined. All the mutant proteins were produced by *Escherichia coli* as C-terminally His_6-tagged proteins. We initially examined the ability of the mutants to bind G-actin (Figure 3). Actin complexed with the His_6-tagged wild-type and mutant cofilin bound to Ni^{2+}–resin. Actin was strictly maintained in a monomeric state by a prior incubation with pancreatic DNase I, an avid actin-sequestering protein that does not interfere with actin binding to cofilin. The results indicated that the affinity of cofilin for G-actin was greatly reduced when Ala was substituted for Ser120 of cofilin. Replacing Tyr82 with Phe slightly weakened the binding, while substituting Ser119 by Ala had no effect. A combination of two or three of these mutations notably affected the affinity.

Cofilin binds to F-actin stoichiometrically and depolymerizes F-actin in a pH-dependent fashion. We determined these activities of the mutants by examining their co-sedimentation with F-actin at two pH values (Figure 4). The co-sedimentation profile of mutant A119 was indistinguishable from that of wild-type cofilin, indicating that the substitution of Ser119 did not affect the activity of cofilin on F-actin. Mutant F82 depolymerized F-actin less efficiently, but co-sedimented with F-actin as efficiently as wild-type cofilin. Taken together with the results shown in Figure 3, the substitution of Tyr82 may

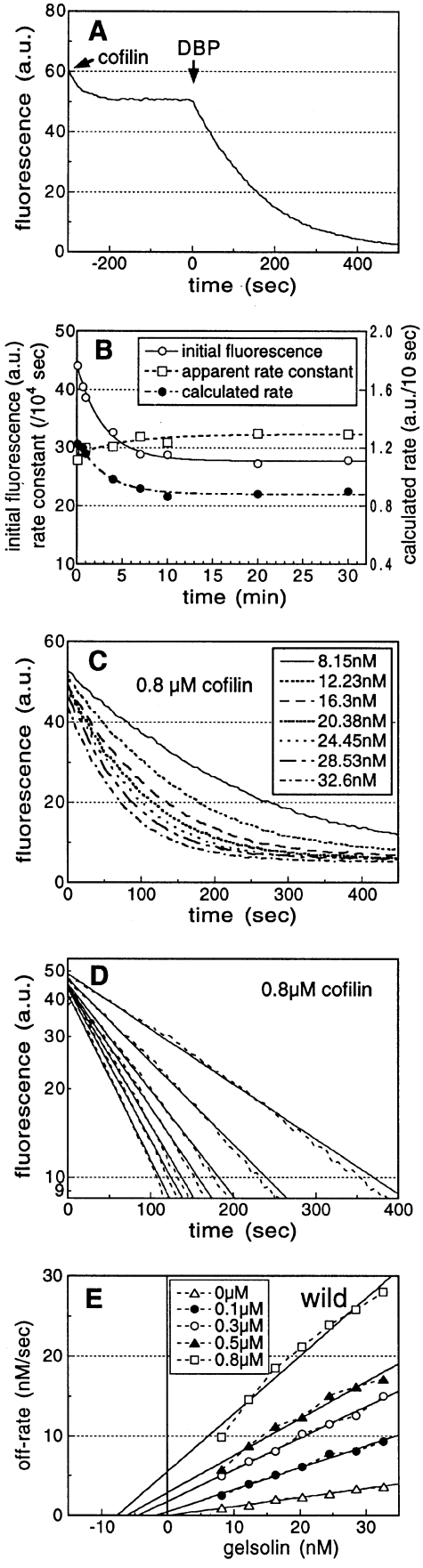

have reduced the affinity of cofilin for monomeric actin, but not for F-actin. Binding to F-actin and the depolymerization activity of mutant A120 were both significantly reduced.

We next examined whether or not these mutations affect the severing of actin filaments and the acceleration of monomer release from their pointed ends. The results indicated that like the wild type, mutant A119 increased the number of filaments (Figure 5B and E) and also accelerated filament disassembly from the pointed end (Figure 5B and D). The acceleration rate caused by mutant F82 was, however, much slower than that of the wild-type cofilin or mutant A119 (Figure 5A and D), which was consistent with its weaker depolymerizing activity (Figure 4). The number of filaments increased with mutant F82, although the extent was moderately reduced (Figure 5A and E). In contrast, mutant A120 (up to 3.6 μM) did not significantly increase the number of filaments, indicating that this mutant had little ability to sever F-actin (Figure 5C and E). The results also showed that this mutant weakly enhanced the disassembly rate (Figure 5C and D). Consistent results for severing were obtained by direct observation of fluorescent F-actin incubated with the mutants under the microscope (Figure 2). Mutant A119 increased the number of filaments almost as efficiently as wild-type cofilin, and mutant F82 produced a moderate increase. However, mutant A120 did not sever F-actin appreciably.

We examined the ability of mutant cofilin to reduce the

Fig. 1. Cofilin increases both the number of pointed ends and the rate of depolymerization from pointed ends of gelsolin-capped actin filaments. (**A**) Schematic representation of the assay to measure the rate of monomer dissociation at the pointed ends in the presence of cofilin. After gelsolin-capped actin filaments (5% pyrene-labelled) were reacted with cofilin for a certain period in the presence of gelsolin–actin dimers, DBP was added and decreasing fluorescence was recorded. (**B**) Dependence of the rate constant for the fluorescence decline on the period of pre-incubation with 0.3 μM His_6-tagged cofilin. The pre-incubation period was varied from 0 to 30 min using 16.3 nM gelsolin-capped filaments (3.3 μM total actin), then the rate constant for the fluorescence decrease was calculated and plotted as a function of the pre-incubation time (□). The fluorescence intensity at the time of DBP addition (○) and the calculated rate of initial fluorescence decrease (●) are also plotted. All three parameters plateaued within 10 min at least in the presence of 0.1–0.8 μM His_6-tagged cofilin. (**C**) Raw data showing fluorescence decline of F-actin (5% pyrene-labelled) after DBP addition. Pyrene–actin was mixed with various concentrations of gelsolin and fully polymerized. After incubation with cofilin for 10 min in the presence of gelsolin–actin dimers, depolymerization was initiated by adding DBP. The initial amount of gelsolin used to construct defined numbers of actin filaments is specified on the graph as the concentration in the final reaction mixture. Final concentrations of cofilin and actin were 0.8 and 3.3 μM, respectively. (**D**) Simulation of the DBP-induced depolymerization processes by adopting exponential kinetics. The end point fluorescence intensity was subtracted from each trace of the fluorescence decrease displayed in (C) and the normalized traces were redrawn on a semi-logarithmic scale (- - - -) and fitted computationally by exponential curves (——). The dotted lines of (D) correspond to traces in (C) from top to bottom. Rate constants were derived from fitted curves. (**E**) Calculated rates of DBP-induced depolymerization plotted as a function of the gelsolin concentration shown in (C). A linear regression fit was applied to each plot. The amount of F-actin at the time of DBP addition was determined as the difference between total actin and actin monomer measured by DNase I inhibition assay. The off-rate (at time = 0) was calculated from the rate constant for the fluorescence decline and the amount of F-actin at the time of DBP addition. The amount of His_6-tagged cofilin is specified as the concentration in the final reaction mixture. The plot of a mock reaction without cofilin is shown as △. Mean values of F-actin concentration at the time of DBP addition were 2.82, 2.56, 2.49, 2.34 and 2.23 μM when cofilin was added at 0, 0.1, 0.3, 0.5 and 0.8 μM, respectively.

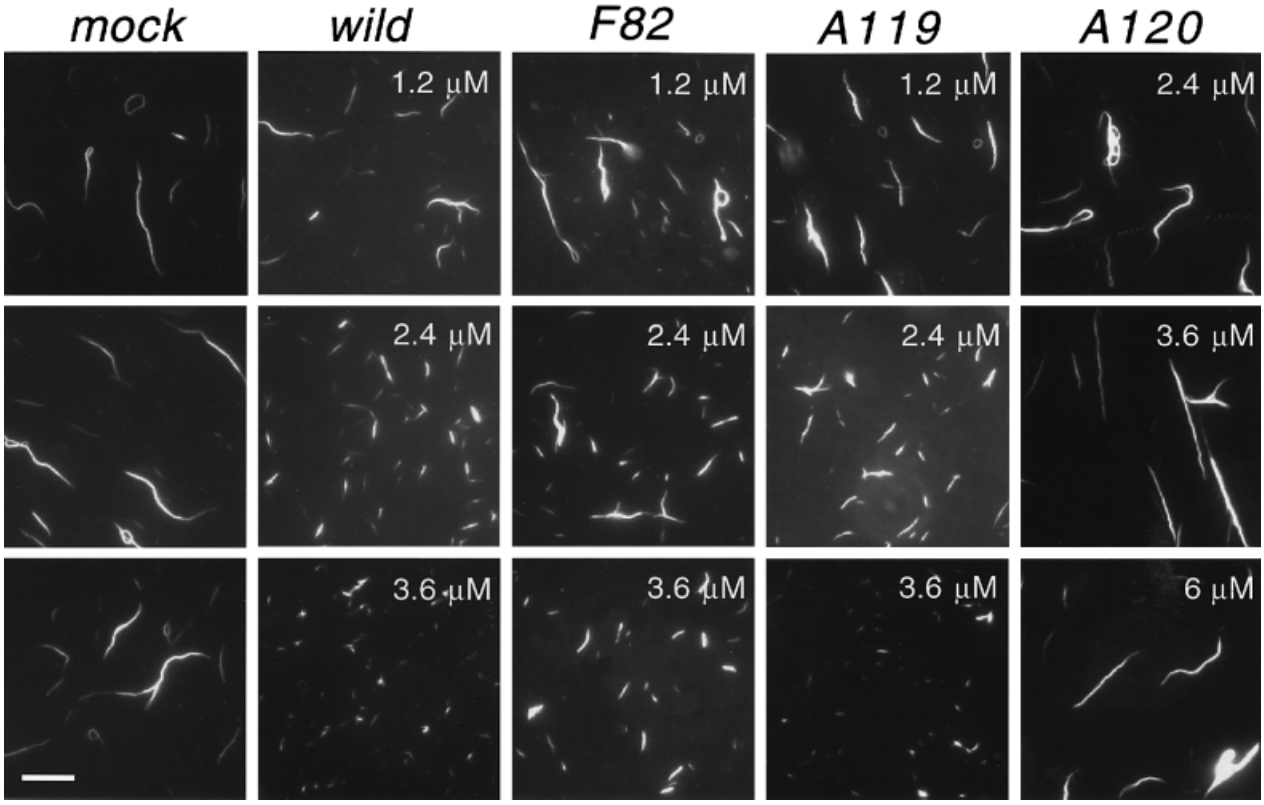

Fig. 2. Microscopic observation of cofilin-induced fragmentation of fluorescently labelled actin filaments. Alexa 488–actin (40% labelled) was polymerized and reacted with various amounts of His_6-tagged cofilin or its mutant at pH 7.0. Cofilin concentrations are specified in each panel; total actin = 2 μM. The mixture was incubated for 20–30 s then examined under an epifluorescence microscope as described in Materials and methods. The bar at bottom left represents 2 μm.

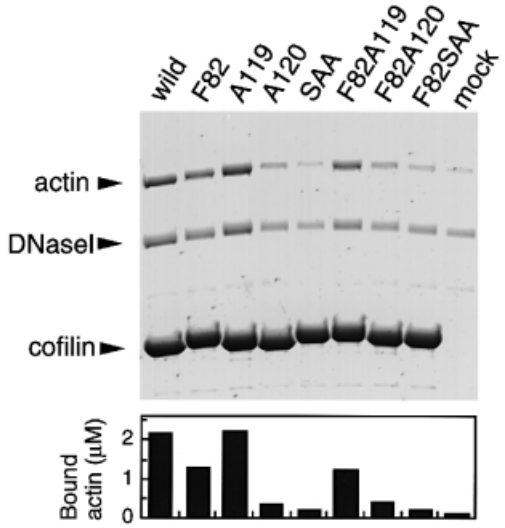

Fig. 3. Ability of cofilin mutants to associate with G-actin. Non-polymerizable complexes of G-actin and DNase I were prepared by incubating 10 μM G-actin with 20 μM DNase I. The mixture was split into aliquots and an equal volume of 30 μM His_6-tagged cofilin or its mutant was added. After 1 h, His_6-tagged proteins and other materials adsorbed to the Ni^{2+}– resin. Upper panel: gel pattern of bound fractions. The amount of bound actin was quantified by densitometry and is shown in the lower panel as a bar graph. SAA, cofilin mutant carrying both A119 and A120 substitutions. F82A119 has both F82 and A119 substitutions. F82A120 and F82SAA are designated accordingly.

viscosity of F-actin solution. Figure 6 shows that mutant A119 reduced the viscosity as efficiently as wild-type cofilin. Mutants F82 and F82A119 also reduced viscosity, but the effective concentrations of these mutants were double that of the wild type. Replacing Ser120 with alanine severely affected this activity. These results are consistent with those of the severing assays presented in Figures 2 and 5.

In vivo effects of mutations A119, F82 and A120

We examined whether or not these mutations affect the biological function of cofilin in living cells. Since cofilin is indispensable for the survival of the budding yeast *Saccharomyces cerevisiae* (Iida *et al*., 1993; Moon *et al*., 1993), we examined the effects of these mutations on the ability of cofilin to support the growth of yeast cells. Porcine cofilin, when expressed by a multicopy plasmid, supports the growth or colony formation of a yeast strain with its *COF1* gene deleted (Figure 7A; Iida *et al*., 1993; Moriyama *et al*., 1996). The F82 and A119 mutants preserved this ability at all temperatures tested (Figure 7A). In contrast, the A120 mutant grew more slowly at 25°C, and was unable to form colonies at higher temperatures (Figure 7A). This did not seem to be caused by reduced structural stability of the A120 protein because the mutant protein was not hypersensitive to unfolding by urea compared with wild-type and other mutant proteins (Figure 8). In addition, the A120 protein was not liable to degradation in yeast cells because the expression level of A120 was 4-fold higher than that of wild-type proteins (data not shown).

In yeast cofilin, Tyr64 corresponds to Tyr82 of porcine cofilin, and Ser103 and Ser104 to Ser119 and Ser120 of porcine cofilin, respectively. We created a set of mutants of the yeast cofilin gene, *COF1*, corresponding to that of the

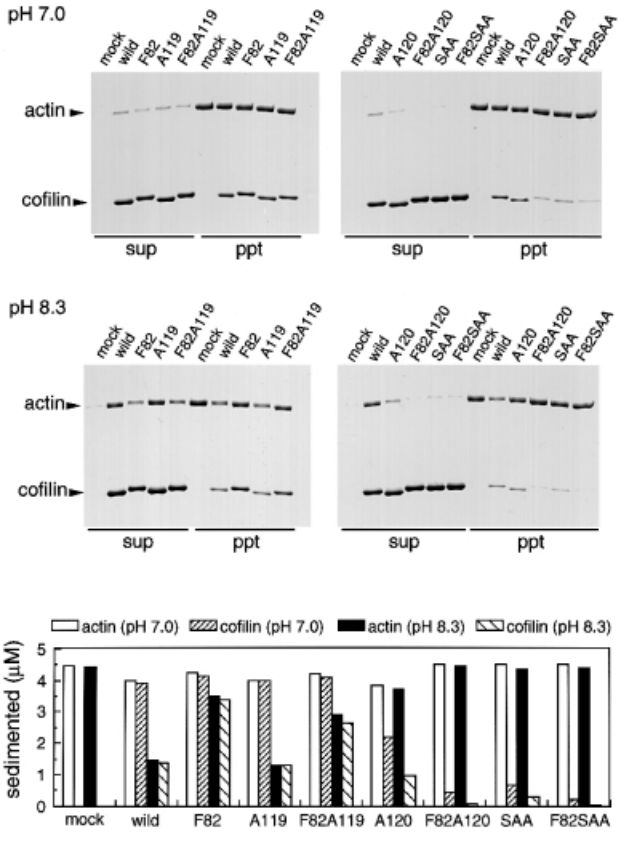

Fig. 4. Ability of cofilin mutants to co-sediment with and depolymerize F-actin. Actin (4.5 μM) was polymerized and reacted with 9.0 μM His_6-tagged cofilin or its mutant for 75 min. F-actin and bound recombinant proteins were sedimented by centrifugation, then supernatant and sediment were resolved by SDS–PAGE. Pairs of upper and middle panels show the results at pH 7.0 and 8.3, respectively. See legend to Figure 3 for mutant designations. The amount of actin and cofilin in the sedimented fraction was quantified and is shown in the lower panel as a bar graph.

pig counterpart. We again examined the ability of these mutants to complement the deletion of *COF1*. A centromere, instead of a multicopy, plasmid was used to express the *cof1* mutant genes. The results showed that all the mutants were viable and that colony size did not differ from that of the wild type under normal growth conditions at 25°C. Mutants carrying the A104 substitution, however, exhibited a temperature-sensitive growth phenotype, as they formed only tiny colonies above 37.5°C (Figure 7B). Thus, conditional growth defects were caused by the A120 substitution of porcine cofilin or a homologous mutation in yeast *COF1*. As characterized above, the A120 mutation impaired severing activity significantly more than it could accelerate directed depolymerization at the pointed end of F-actin, whereas the F82 mutation considerably reduced the latter activity with a smaller effect on severing. The F82 substitution of porcine cofilin or a homologous substitution in yeast *COF1* had no apparent adverse effect on yeast growth.

These results suggest that filament-severing activity is at least important for cofilin to sustain yeast growth. The activity of cofilin in enhancing directed depolymerization may also play a physiological role in cooperation with its severing activity.

Discussion

Dual functions of cofilin

Whether or not cofilin severs F-actin has been controversial since Carlier *et al*. (1997) claimed that cofilin/ADF does not sever, but exclusively accelerates the treadmilling of F-actin. We describe here an improved method to measure fragmentation and the dissociation rate constant at the pointed end of F-actin in the presence of a substoichiometric amount of cofilin. When the barbed end of F-actin is capped, total disassembly must depend on the off-rate at the pointed end and the number of filaments per unit volume. The latter must be increased by severing events, if they occur, with cofilin. A relatively rapid quenching phase was not easily separated from a depolymerization phase if cofilin and DBP were added simultaneously to pyrene-labelled F-actin. In addition, our calibration predicted a stoichiometric (non-catalytic) nature of filament severing by cofilin, which apparently ceased within 10 min. We therefore initiated DBP-induced depolymerization after a 10 min incubation with cofilin, during which the level of fluorescence reduction reached a plateau. The kinetics of DBP-induced depolymerization processes was also consistent with the non-catalytic model of severing by cofilin. F-actin depolymerization follows exponential kinetics if the filament length distribution is exponential. This is true for either spontaneously polymerized or gelsolin-nucleated filaments (Kawamura and Maruyama, 1972; Bryan and Coluccio, 1985; Janmey *et al*., 1986). If fragmentation of the filaments continues during the DBP-induced depolymerization phase, a semilog plot of depolymerization could give a downward curvature according to gradual increases in the number of filament ends. In practice, a large part of the depolymerization plot agreed with an exponential curve in the presence or absence of cofilin. We observed a negligible downward curvature even in the presence of 0.8 μM cofilin (the highest concentration used in this assay; Figure 1D). This suggested little recurrent severing during induced depolymerization. Other reports also suggest a non-catalytic nature of severing by cofilin/ADF family proteins (Hayden *et al*., 1993; Maciver *et al*., 1998; Blanchoin and Pollard, 1999).

Carlier *et al*. (1997) demonstrated that ADF accelerates depolymerization from pointed ends of actin filaments as much as 22-fold. The results obtained with wild-type cofilin shown in Figure 1E indicate that cofilin at substoichiometric doses also accelerates their disassembly at the pointed end. However, we could only observe up to a 6.4-fold increase, since the methodology restricted the use of higher cofilin doses. Another potential problem is related to a recent report arguing that gelsolin-capped, short filaments are resistant to severing by cofilin/ADF family proteins (Maciver *et al*., 1998). If gelsolin-capped, shorter filaments are less susceptible to severing by cofilin, we might have overestimated the severing efficiency and underestimated the dissociation rate constant at the pointed end. However, Maciver *et al*. (1998) used as much as 5% gelsolin/actin for preparing gelsolin-capped filaments, whereas we used only 0.24–0.99% gelsolin/actin. In addition, most of our plots of off-rate versus gelsolin (Figures 1E and 5A–C) show little trend of convexity, which would be expected if gelsolin-capped, shorter filaments were more resistant to severing by cofilin. Hence, our measurements of the two parameters are reasonably valid at least at this lower ratio of gelsolin/

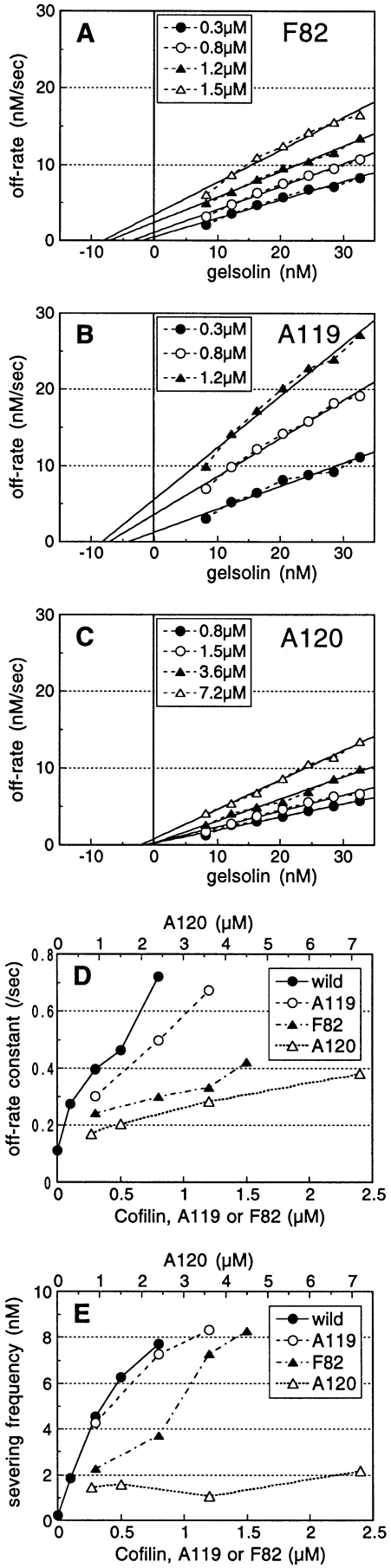

actin and at relatively low concentrations of cofilin. Future improvements to the method would allow similar analyses for higher cofilin concentrations.

Didry *et al.* (1998) demonstrated that the number of filaments increased in the presence of plant ADF. However, they argued that this was due to a readjustment of the filament length distribution, caused by enhanced F-actin turnover, and that it was unlikely to be a result of severing. If this was true, the increase in filaments could be paralleled by the acceleration of depolymerization at the pointed ends. In contrast, we found little correlation between these two activities in the cofilin mutants F82 and A120 (Figure 5D and E). Hence, most of the observed increases in the number of filaments must be the result of severing.

Structural and functional roles for a triad of hydrogen bonds in cofilin

While cofilin and gelsolin have quite distinct primary structures, unitary segments of gelsolin are similar to cofilin in tertiary structure (Hatanaka *et al.*, 1996; Fedorov *et al.*, 1997; Leonard *et al.*, 1997). The actin-binding sites of cofilin have been mapped to/around its longest helix, and the corresponding helix of the first segment of gelsolin also

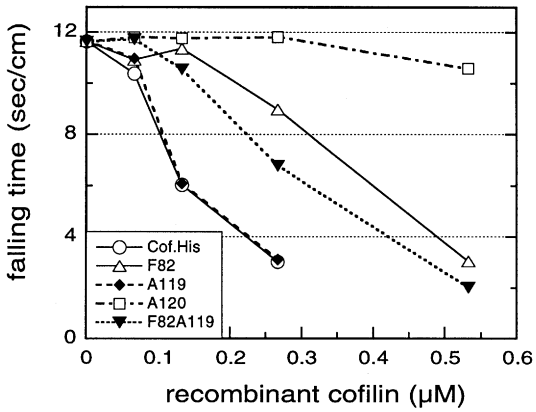

Fig. 6. Effect of cofilin mutants on viscosity of F-actin solution. Low-shear viscosity of the solution was assessed using a miniature falling ball apparatus. Actin (3.5 μM) was polymerized in 50 μl capillary tubes in the presence of various concentrations of His_6-tagged cofilin or its mutants at pH 7.5. Viscosity was measured after 5 h of polymerization and is represented as the mean time required by the ball to fall by 1 cm.

Fig. 5. Ability of cofilin mutant proteins to increase the number of filaments and to accelerate directed depolymerization of gelsolin-capped actin filaments. Porcine cofilin mutants A119, F82 and A120 were assayed as detailed for wild-type cofilin in Figure 1. (**A–C**) Plots of calculated depolymerization rate versus initial gelsolin concentration for mutants F82 (A), A119 (B) and A120 (C). Mean values of F-actin concentration at the time of DBP addition were 2.73, 2.49, 2.25 and 2.05 μM when mutant F82 was used at 0.3, 0.8, 1.2 and 1.5 μM, respectively. These values were 2.57, 2.39 and 2.17 μM when mutant A119 was used at 0.3, 0.8 and 1.2 μM, respectively. Values were 2.71, 2.67, 2.62 and 2.43 μM when mutant A120 was used at 0.8, 1.5, 3.6 and 7.2 μM, respectively. (**D**) Rate constants for monomer dissociation at the pointed end were read from slopes of linear regression lines in (A–C), then plotted as a function of concentration of cofilin mutant proteins. The plot for wild-type cofilin was derived from Figure 1E. (**E**) Increments in the number (concentration) of filaments were read from the intercept of the linear regression lines with the horizontal axis in (A–C), and plotted against concentrations of cofilin mutant proteins. Plots for the wild type are derived from Figure 1E in (D) and (E). The abscissa scales for the A120 mutant (top scale) and for the others (bottom scale) are different in (D) and (E).

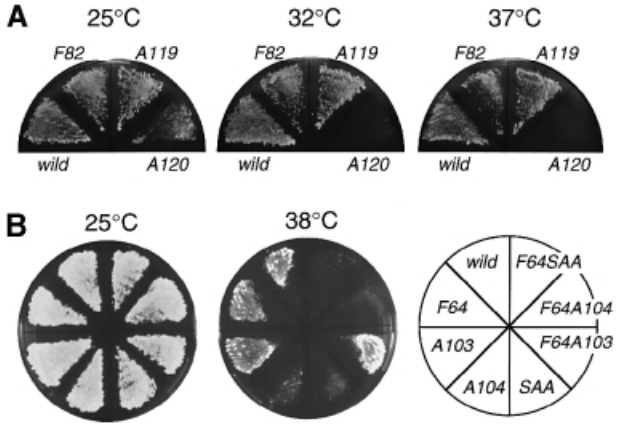

Fig. 7. The A120 substitution of porcine cofilin and analogous substitution in *COF1* conferred thermosensitivity upon *S.cerevisiae*. (**A**) Yeast strains carrying multicopy plasmids expressing porcine cofilin mutants were created by a standard plasmid-shuffling protocol. All three mutants compensated for the loss of the chromosomal *COF1* gene at 25°C. These strains were examined for colony formation at 25 (left), 32 (middle) and 37°C (right). Photographs were taken after 6 days for the A120 mutant and after 4 days for the other mutants. (**B**) Yeast strains carrying centromere plasmids carrying the mutant *cof1* gene were created similarly. Mutant strains were examined for colony formation between 18 and 38°C. The results at 25 (left) and 38°C (middle) are presented together with a diagram (right) showing the location of mutant strains on agar plates. SAA is a *COF1* mutant carrying both A103 and A104 substitutions. F64A103 has both F64 and A103 substitutions. F64A104 and F64SAA are designated accordingly. Photographs were taken after 3 days at 25°C (left) or after 6 days at 38°C (middle).

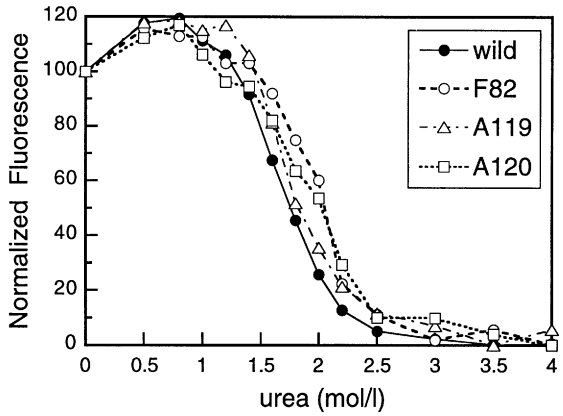

Fig. 8. Structural stability of the cofilin mutant proteins. Recombinant wild-type or mutant cofilin (1.5 μM) was incubated in the presence of various amounts of urea for 60 min, then the intrinsic fluorescence was measured, normalized and plotted as a function of urea concentration.

constitutes its primary contact with actin (McLaughlin *et al*., 1993). Thus, cofilin may assume a tertiary structure similar to that of the first or fourth segment of gelsolin when bound to actin. Despite this similarity, their modes of interaction with actin differ. For instance, segment 1 caps F-actin, whereas cofilin does not. Cofilin binds along F-actin then severs it, whereas segment 1 does not. Considering the structural differences, the long helix of cofilin is markedly kinked in contrast to those of the actin-binding segments of gelsolin. Although segments 3 and 6 of gelsolin have kinked helices, they are not thought to bind actin directly (Burtnick *et al*., 1997; McGough *et al*., 1998). The triad of hydrogen bonds on the actin-binding helix of cofilin must contribute to the formation of the kink, prompting an investigation of their functional significance. This study revealed a central role for the hydrogen bond between the backbone carbonyl of Ile116 and the side chain hydroxyl of Ser120 located at the centre of the triad in porcine cofilin. Replacement of Ser120 with alanine significantly reduced its severing activity. The same mutation also weakened the ability of cofilin to bind along F-actin and the accelerated depolymerization from the pointed end. The F82 mutation impaired the pH-dependent actin-depolymerizing activity of cofilin, suggesting that a hydrogen bond between the side chain hydroxyl of Tyr82 and the backbone carbonyl of Tyr117 is another structural element for the unique functional fold in the actin-binding helix of cofilin.

Jiang *et al*. (1997) presented a contradictory report about a mutation of the equivalent tyrosine residue of a maize isoform of ADF/cofilin (ZmADF3). However, they worked with a double mutant and did not verify whether an F82-equivalent mutation was responsible for the contradictory effect. We surmise that the side effects of the other mutation would have interfered with their evaluation of the role of Tyr82.

Role of the triad of hydrogen bonds in vital functions of cofilin

This study demonstrated that two hydrogen bonds out of the triad are structural factors that modulate the biochemical activities of cofilin, including F-actin severing and acceleration of its directed subunit release. The central hydrogen bond is a primary element for both activities, while that involving Tyr82 is responsible for accelerating depolymerization rather than for severing. This finding also suggests that the kink in the actin-binding helix of cofilin has functional significance. Other mutational studies of cofilin/ADF in nematodes and yeast also mapped the important residues to the middle of the actin-binding helix (Iida and Yahara, 1999; Ono *et al*., 1999).

On the other hand, the mutational elimination of hydrogen bonds within the triad did not prevent normal cell growth (Figure 7), suggesting that a partial reduction in the activities of cofilin is not critical for ordinary growth. However, a conditional growth defect was conferred by the A120 substitution of porcine cofilin or the A104 substitution in yeast *COF1*, which disrupted the central hydrogen bond of the triad. Comparing this phenotype with the reduced biochemical activities of the A120 mutant suggests that the severing activity mediates vital functions of cofilin *in vivo*. In contrast, the F82 substitution of porcine cofilin or the F64 substitution in yeast *COF1* did not seem to affect cell growth. As the F82 mutation impaired the accelerated actin dissociation at the pointed end much more than the severing activity, the ability of cofilin to accelerate directed depolymerization and the consequent acceleration of treadmilling in F-actin may be less important for yeast growth than filament severing. Alternatively, the reduced ability to accelerate treadmilling in these yeast mutants might be compensated by another cellular factor(s) that could cooperate with cofilin in yeast cells. Thus, the physiological significance of this activity might have been overlooked in our experiments. Although our results are consistent with the notion that the cofilin/ADF-induced acceleration of

directed disassembly of actin filaments is primarily responsible for the rapid turnover of F-actin, they further suggest that the severing activity of cofilin is physiologically important.

Materials and methods

Proteins and reagents

Actin was purified from rabbit skeletal muscle by the method of Spudich and Watt (1971), then gel-filtrated on Sephacryl S-200 equilibrated with G-buffer [2 mM Tris–HCl, 0.1 mM $CaCl_2$, 0.2 mM ATP, 0.1 mM dithiothreitol (DTT), 0.01% NaN_3 pH 7.8]. Gelsolin was purified from bovine plasma according to the method of Kurokawa *et al*. (1990). Human DBP was purchased from Calbiochem-Novabiochem Co. (La Jolla, CA). Alexa 488-labelled actin and *N*-(1-pyrenyl)iodoacetamide were obtained from Molecular Probes, Inc. (Eugene, OR). Pyrenyl–actin was prepared by the method of Kouyama and Mihashi (1981). Calcium-actin was converted into Mg-actin during a 3 min incubation in the presence of 0.2 mM EGTA and a 1 M equivalent plus a 10 μM excess of $MgCl_2$ at room temperature. All other chemicals were of analytical grade.

Plasmid construction and protein expression

DNA was manipulated conventionally according to Sambrook *et al*. (1989). Site-specific mutations were generated by the two-step PCR protocol (Kuipers *et al*., 1991). Cofilin mutant proteins were expressed in *E.coli* BL21(Rep4) and purified as described (Moriyama *et al*., 1996). A His_6 tag was added to the C-terminus of every recombinant cofilin. For the yeast study, we used the multicopy plasmid, YEplac181, and the centromere plasmid, YCplac111 (Gietz and Sugino, 1988). The authentic cofilin gene of *S.cerevisiae*, *COF1*, was modified as described (Moriyama *et al*., 1996); a unique intron was removed and *Nco*I and *Bam*HI sites were introduced at the beginning and end of the open reading frame (ORF), respectively. A 1.2 kbp *Eco*RI–*Sph*I fragment of the modified *COF1* gene was then inserted into YEplac181 or YCplac111. The ORF of *COF1* on YEplac181 was replaced with that of porcine cofilin mutants, and the ORF on YCplac111 was replaced with that of *COF1* mutants.

Measurement of depolymerization rates at pointed filament ends

Calcium-G-actin (5% pyrenyl-labelled) was incubated for 3 min in the presence of a 1 M equivalent plus a 10 μM excess of $MgCl_2$ at room temperature, then mixed with various concentrations of gelsolin. Polymerization was initiated by adding $MgCl_2$ and KCl to 2 and 100 mM, respectively. Although we usually add EGTA to convert Ca-actin into Mg-actin before polymerization, the same handling in the presence of gelsolin produced deviations in the resulting number of filaments (estimated from the depolymerization rate) possibly because of inefficient nucleation by gelsolin. Thus, we omitted EGTA and this resulted in better correlation of the depolymerization rate with the gelsolin concentration. The polymerized filaments consequently would consist of both Ca- and Mg-actins. After 3 h of polymerization at 28°C, His_6-tagged cofilin and gelsolin–actin dimers (20 nM) were added simultaneously and reacted for 10 min, during which a new steady-state was reached in pyrene fluorescence. The binary complex of gelsolin and actin should cap the free barbed ends generated by the severing action of cofilin. DBP, a potent actin-sequestering agent, was added to induce depolymerization of the filaments. Gradual changes in fluorescence intensity were monitored immediately. The dead-time was 4–8 s and the final concentrations of actin and DBP were 3.3 and 3.5 μM, respectively. Depolymerization proceeded in 120 μl of 6.6 mM Tris–HCl, 14.6 mM HEPES–KOH, 2 mM $MgCl_2$, 100 mM KCl, 85 μM ATP, 0.51 mM EGTA, 15 μM $CaCl_2$, 0.18 mM DTT at pH 7.1. End point fluorescence intensity was measured after overnight reactions. Fluorescence data were collected at 25°C using a Perkin-Elmer LS-50B Luminescence spectrophotometer. The wavelengths for excitation and emission were 365 and 407 nm, respectively.

Analysis of depolymerization kinetics

To calculate the rate of monomer dissociation from actin filaments, the total amount of F-actin at the time of DBP addition must be determined. The amount of F-actin was calculated by subtracting that of monomeric actin from the total amount of actin after the monomer was quantified by a DNase I inhibition assay (see below). Fluorescence intensity was converted to the concentration of F-actin for each kinetic assay, since both the initial and final (end point) intensities of the pyrene fluorescence were known. The amount of F-actin per fluorescence unit depended significantly on the concentration of cofilin, but relatively little on that of gelsolin. Thus, the initial rate of depolymerization was calculated from that of the fluorescence decrease and plotted against the initial concentration of gelsolin ($= N_o$ in the following equations), which equals the initial number of filaments (Bryan and Coluccio, 1985; Janmey *et al*., 1986; Weber *et al*., 1994). In practice, most of the fluorescence intensity declined following exponential kinetics, indicating that the filament length distribution is exponential and that little fragmentation of F-actin continues during DBP-induced depolymerization. We therefore calculated the rate constant by adopting an exponential curve fitting to the disassembly trace as far as when 80% of F-actin disappeared. Then, the off-rate (at time = 0) was obtained as a product of the calculated rate constant and the initial concentration of F-actin. This procedure precluded an ambiguous definition of the off-rate.

Under a defined concentration of cofilin and assuming that filament severing by cofilin was stoichiometric, an apparent rate constant for the dissociation of the actin subunit from a pointed end and the number of severing events can be calculated as follows. If n cuts per unit volume are administered to gelsolin-capped actin filaments, the number (concentration) of filament ends will be

$$N_p = N_o + n \quad (1)$$

$$N_b = n \quad (2)$$

where N_o is the initial number of filaments, and N_p and N_b are the numbers of free pointed and barbed ends, respectively. We only considered the reaction at pointed ends, since barbed ends should be capped by gelsolin–actin dimers. The back reaction, or subunit addition to filament ends, can also be neglected because it was eventually prevented under our experimental conditions. Hence, the off-rate was directly proportional to N_p, and is expressed as

$$V_i = k_{p-}N_p = k_{p-}(N_o + n) \quad (3)$$

where V_i is the initial rate of DBP-induced depolymerization and k_{p-} is the apparent rate constant for subunit dissociation at the pointed end. As described in Results, k_{p-} is dependent on the amount of cofilin. According to Equation 3, the plot of V_i versus N_o should give a linear regression line with a slope k_{p-} that should intersect with the horizontal axis at $-n$.

More precisely, N_o in the plot needs to be corrected, because it decreases during the pre-incubation with cofilin under the assumption that the filament length distribution is exponential. We replotted the data taking this into account, and found that the results were essentially similar to those using original N_o, unless >1.4 μM actin was depolymerized before DBP addition. For this reason, we presented the plots without the correction for N_o to simplify understanding of our results.

General biochemical assay for cofilin activities

Monomeric actin just before the DBP induction of depolymerization was quantified by the DNase I inhibition assay (Blikstad *et al*., 1978) as modified by Harris *et al*. (1982). Co-sedimentation assays proceeded as described (Moriyama *et al*., 1996). The ability of His_6-tagged cofilin and its mutant to associate with DNase I-bound G-actin was assessed using Ni^{2+}–nitrilotriacetic acid–Sepharose CL-6B (Qiagen Inc., Chatsworth, CA). This assay was performed as described (Moriyama *et al*., 1996) except that DNase I–actin complex was used instead of free G-actin in the present study. Bands in polyacrylamide gels were quantified using a PDI420oe scanning densitometer and Quantity One Software (PDI Inc., New York, NY). Falling ball viscometry was performed as described (Aizawa *et al*., 1995).

Direct observation of filamentous actin

Alexa 488–actin (40% labelled) was converted to its Mg^{2+} form and polymerized for 2 h. Various concentrations of His_6-tagged cofilin in 3 μl were added to 2 μl of 5 μM polymerized Alexa–actin. The mixture consisting of 2 μM F-actin, 20 mM PIPES–KOH, 8.8 mM Tris–HCl, 0.8 mM $MgCl_2$, 0.02 mM $CaCl_2$, 100 mM KCl, 0.08 mM EGTA and 0.42 mM DTT (pH 7.0) was incubated for 20–30 s, then 15 μl of mounting medium, PermaFluor (Immunon, Pittsburgh, PA), were added. A 4 μl aliquot was placed onto a glass slide, coverslipped, and immediately observed under a Carl Zeiss epifluorescence microscope (Axiophot) equipped with a 100× oil immersion objective. Microscope images were captured on a cooled CCD camera C4880 (Hamamatsu Photonics, Shizuoka, Japan) and recorded by an Argus-50 image processor (Hamamatsu Photonics).

Urea denaturation assay

His_6-tagged wild-type or mutant cofilin (1.5 μM) was incubated with various amounts of urea in 20 mM Tris–HCl, 0.2 mM DTT (pH 7.5) at

room temperature for 60 min, then intrinsic fluorescence was measured at an excitation of 280 nm and emission of 330 nm. The data were normalized and plotted as a function of the urea concentration.

Complementation assay in S.cerevisiae

Whether or not mutant cofilin can functionally replace authentic cofilin in *S.cerevisiae* was determined by plasmid shuffling as described (Moriyama *et al*., 1996). Strain HE8 (*MAT***a** *leu2 ura3 trp1 his3 cof1*Δ*::HIS3* + YCpYCS*/COF1/URA3/CEN*) was transformed with a YCplac111-based plasmid carrying mutated *cof1* and a selectable *LEU2* marker. Next, cells that have lost YCpYCS were selected using 5-fluoro-orotic acid. All cofilin mutants tested here compensated for the lost *COF1* gene. The thermosensitivity of each mutant strain was examined by streaking the colonies onto SC plates lacking leucine and histidine, then incubating them at various temperatures for 3–6 days. To examine heterologous complementation by mutated porcine cofilin, we used a YEplac181- instead of a YCplac111-based plasmid.

Acknowledgements

We are very grateful to Dr H.Hatanaka (our institution) for providing unpublished data on the hydrogen bond involving Tyr82 of destrin. We also thank Drs H.Aizawa and K.Iida (our laboratory) for technical advice and encouragement. This work was supported by a Grant-in-Aid for Specially Promoted Research (09101002) from the Ministry of Education, Science and Culture of Japan.

References

Abe,H., Obinata,T., Minamide,L.S. and Bamburg,J.R. (1996) *Xenopus laevis* actin-depolymerizing factor/cofilin: a phosphorylation-regulated protein essential for development. *J. Cell Biol.*, **132**, 871–885.

Aizawa,H., Sutoh,K., Tsubuki,S., Kawashima,S., Ishii,A. and Yahara,I. (1995) Identification, characterization and intracellular distribution of cofilin in *Dictyostelium discoideum*. *J. Biol. Chem.*, **270**, 10923–10932.

Aizawa,H., Sutoh,K. and Yahara,I. (1996) Overexpression of cofilin stimulates bundling of actin filaments, membrane ruffling and cell movement in *Dictyostelium*. *J. Cell Biol.*, **132**, 335–344.

Blanchoin,L. and Pollard,T.D. (1999) Mechanism of interaction of *Acanthamoeba* actophorin (ADF/cofilin) with actin filaments. *J. Biol. Chem.*, **274**, 15538–15546.

Blikstad,I., Markey,F., Carlsson,L., Persson,T. and Lindberg,U. (1978) Selective assay of monomeric and filamentous actin in cell extracts, using inhibition of deoxyribonuclease I. *Cell*, **15**, 935–943.

Bryan,J. and Coluccio,L.M. (1985) Kinetic analysis of F-actin depolymerization in the presence of platelet gelsolin and gelsolin–actin complexes. *J. Cell Biol.*, **101**, 1236–1244.

Burtnick,L.D., Koepf,E.K., Grimes,J., Jones,E.Y., Stuart,D.I., McLaughlin,P.J. and Robinson,R.C. (1997) The crystal structure of plasma gelsolin: implications for actin severing, capping and nucleation. *Cell*, **90**, 661–670.

Carlier,M.F., Laurent,V., Santolini,J., Melki,R., Didry,D., Xia,G.X., Hong,Y., Chua,N.H. and Pantaloni,D. (1997) Actin depolymerizing factor (ADF/cofilin) enhances the rate of filament turnover: implication in actin-based motility. *J. Cell Biol.*, **136**, 1307–1322.

Didry,D., Carlier,M.F. and Pantaloni,D. (1998) Synergy between actin depolymerizing factor/cofilin and profilin in increasing actin filament turnover. *J. Biol. Chem.*, **273**, 25602–25611.

Fedorov,A.A., Lappalainen,P., Fedorov,E.V., Drubin,D.G. and Almo,S.C. (1997) Structure determination of yeast cofilin. *Nature Struct. Biol.*, **4**, 366–369.

Gietz,R.D. and Sugino,A. (1988) New yeast–*Escherichia coli* shuttle vectors constructed with *in vitro* mutagenized yeast genes lacking six-base pair restriction sites. *Gene*, **74**, 527–534.

Gunsalus,K.C., Bonaccorsi,S., Williams,E., Verni,F., Gatti,M. and Goldberg,M.L. (1995) Mutations in *twinstar*, a *Drosophila* gene encoding a cofilin/ADF homologue, result in defects in centrosome migration and cytokinesis. *J. Cell Biol.*, **131**, 1243–1259.

Harris,H.E., Bamburg,J.R., Bernstein,B.W. and Weeds,A.G. (1982) The depolymerization of actin by specific proteins from plasma and brain: a quantitative assay. *Anal. Biochem.*, **119**, 102–114.

Hatanaka,H., Ogura,K., Moriyama,K., Ichikawa,S., Yahara,I. and Inagaki,F. (1996) Tertiary structure of destrin and structural similarity between two actin-regulating protein families. *Cell*, **85**, 1047–1055.

Hayden,S.M., Miller,P.S., Brauweiler,A. and Bamburg,J.R. (1993) Analysis of the interactions of actin depolymerizing factor with G- and F-actin. *Biochemistry*, **32**, 9994–10004.

Iida,K. and Yahara,I. (1999) Cooperation of two actin-binding proteins, cofilin and Aip1, in *Saccharomyces cerevisiae*. *Genes Cells*, **4**, 21–32.

Iida,K., Moriyama,K., Matsumoto,S., Kawasaki,H., Nishida,E. and Yahara,I. (1993) Isolation of a yeast essential gene, *COF1*, that encodes a homologue of mammalian cofilin, a low-M_r actin-binding and depolymerizing protein. *Gene*, **124**, 115–120.

Janmey,P.A., Peetermans,J., Zaner,K.S., Stossel,T.P. and Tanaka,T. (1986) Structure and mobility of actin filaments as measured by quasielastic light scattering, viscometry and electron microscopy. *J. Biol. Chem.*, **261**, 8357–8362.

Jiang,C.J., Weeds,A.G., Khan,S. and Hussey,P.J. (1997) F-actin and G-actin binding are uncoupled by mutation of conserved tyrosine residues in maize actin depolymerizing factor (ZmADF). *Proc. Natl Acad. Sci. USA*, **94**, 9973–9978.

Kawamura,M. and Maruyama,K. (1972) A further study of electron microscopic particle length of F-actin polymerized *in vitro*. *J. Biochem.*, **72**, 179–188.

Kouyama,T. and Mihashi,K. (1981) Fluorimetry study of *N*-(1-pyrenyl)-iodoacetamide-labelled F-actin. Local structural change of actin protomer both on polymerization and on binding of heavy meromyosin. *Eur. J. Biochem.*, **114**, 33–38.

Kuipers,O.P., Boot,H.J. and de Vos,W.M. (1991) Improved site-directed mutagenesis method using PCR. *Nucleic Acids Res.*, **19**, 4558.

Kurokawa,H., Fujii,W., Ohmi,K., Sakurai,T. and Nonomura,Y. (1990) Simple and rapid purification of brevin. *Biochem. Biophys. Res. Commun.*, **168**, 451–457.

Lappalainen,P. and Drubin,D.G. (1997) Cofilin promotes rapid actin filament turnover *in vivo*. *Nature*, **388**, 78–82.

Leonard,S.A., Gittis,A.G., Petrella,E.C., Pollard,T.D. and Lattman,E.E. (1997) Crystal structure of the actin-binding protein actophorin from *Acanthamoeba*. *Nature Struct. Biol.*, **4**, 369–373.

Maciver,S.K., Zot,H.G. and Pollard,T.D. (1991) Characterization of actin filament severing by actophorin from *Acanthamoeba castellanii*. *J. Cell Biol.*, **115**, 1611–1620.

Maciver,S.K., Pope,B.J., Whytock,S. and Weeds,A.G. (1998) The effect of two actin depolymerizing factors (ADF/cofilins) on actin filament turnover: pH sensitivity of F-actin binding by human ADF, but not of *Acanthamoeba* actophorin. *Eur. J. Biochem.*, **256**, 388–397.

McGough,A., Chiu,W. and Way,M. (1998) Determination of the gelsolin binding site on F-actin: implications for severing and capping. *Biophys. J.*, **74**, 764–772.

McKim,K.S., Matheson,C., Marra,M.A., Wakarchuk,M.F. and Baillie,D.L. (1994) The *Caenorhabditis elegans unc-60* gene encodes proteins homologous to a family of actin-binding proteins. *Mol. Gen. Genet.*, **242**, 346–357.

McLaughlin,P.J., Gooch,J.T., Mannherz,H.G. and Weeds,A.G. (1993) Structure of gelsolin segment 1–actin complex and the mechanism of filament severing. *Nature*, **364**, 685–692.

Moon,A.L., Janmey,P.A., Louie,K.A. and Drubin,D.G. (1993) Cofilin is an essential component of the yeast cortical cytoskeleton. *J. Cell Biol.*, **120**, 421–435.

Moriyama,K., Yonezawa,N., Sakai,H., Yahara,I. and Nishida,E. (1992) Mutational analysis of an actin-binding site of cofilin and characterization of chimeric proteins between cofilin and destrin. *J. Biol. Chem.*, **267**, 7240–7244.

Moriyama,K., Iida,K. and Yahara,I. (1996) Phosphorylation of Ser-3 of cofilin regulates its essential function on actin. *Genes Cells*, **1**, 73–86.

Nishida,E., Maekawa,S. and Sakai,H. (1984) Cofilin, a protein in porcine brain that binds to actin filaments and inhibits their interactions with myosin and tropomyosin. *Biochemistry*, **23**, 5307–5313.

Nishida,E., Muneyuki,E., Maekawa,S., Ohta,Y. and Sakai,H. (1985) An actin-depolymerizing protein (destrin) from porcine kidney. Its action on F-actin containing or lacking tropomyosin. *Biochemistry*, **24**, 6624–6630.

Ono,S., Baillie,D.L. and Benian,G.M. (1999) UNC-60B, an ADF/cofilin family protein, is required for proper assembly of actin into myofibrils in *Caenorhabditis elegans* body wall muscle. *J. Cell Biol.*, **145**, 491–502.

Rosenblatt,J., Agnew,B.J., Abe,H., Bamburg,J.R. and Mitchison,T.J. (1997) *Xenopus* actin depolymerizing factor/cofilin (XAC) is responsible for the turnover of actin filaments in *Listeria monocytogenes* tails. *J. Cell Biol.*, **136**, 1323–1332.

Sambrook,J., Fritsch,E.F. and Maniatis,T. (1989) *Molecular Cloning: A Laboratory Manual.* 2nd edn. Cold Spring Harbor Laboratory Press, Cold Spring Harbor, NY.

Spudich,J.A. and Watt,S. (1971) The regulation of rabbit skeletal muscle

contraction. I. Biochemical studies of the interaction of the tropomyosin–troponin complex with actin and the proteolytic fragments of myosin. *J. Biol. Chem.*, **246**, 4866–4871.

Walsh,T.P., Weber,A., Higgins,J., Bonder,E.M. and Mooseker,M.S. (1984) Effect of villin on the kinetics of actin polymerization. *Biochemistry*, **23**, 2613–2621.

Weber,A., Pennise,C.R. and Pring,M. (1994) DNase I increases the rate constant of depolymerization at the pointed (–) end of actin filaments. *Biochemistry*, **33**, 4780–4786.

Wriggers,W., Tang,J.X., Azuma,T., Marks,P.W. and Janmey,P.A. (1998) Cofilin and gelsolin segment-1: molecular dynamics simulation and biochemical analysis predict a similar actin binding mode. *J. Mol. Biol.*, **282**, 921–932.

Yonezawa,N., Nishida,E., Ohba,M., Seki,M., Kumagai,H. and Sakai,H. (1989) An actin-interacting heptapeptide in the cofilin sequence. *Eur. J. Biochem.*, **183**, 235–238.

Yonezawa,N., Nishida,E., Iida,K., Kumagai,H., Yahara,I. and Sakai,H. (1991) Inhibition of actin polymerization by a synthetic dodecapeptide patterned on the sequence around the actin-binding site of cofilin. *J. Biol. Chem.*, **266**, 10485–10489.

Received January 25, 1999; revised and accepted October 4, 1999